Efficient numerical modelling of non-isothermal viscoelastic fluids

Stefanie Meburger[1,2] and Michael Schäfer[1,2]

[1] Department of Numerical Methods in Mechanical Engineering, TU Darmstadt
[2] Graduate School of Computational Engineering, TU Darmstadt
Dolivostr. 15, 64293 Darmstadt, Germany

ABSTRACT

In this numerical study the flow behavior of a viscoelastic Oldroyd-B fluid in a 4:1 planar contraction flow is investigated under non-isothermal conditions. The approach is based upon the Finite-Volume-Method. Important flow characteristica like dimensionless stress and velocity profiles and the corner vortex size are analyzed and compared to literature data.

INTRODUCTION

Non-isothermal flow of viscoelasic fluids may be encountered in many real-life applications. The manufacturing process of polymers is one well-established example. Since the 1950s the interest to describe these fluids analytically and to solve the resulting set of equations numerically has been growing continuously. The common aim in most of the publications on the subject is to gain a deeper understanding of the underlying processes. This understanding might help to treat the material more effectively and also reduce waste.[17]

The 4:1 contraction flow is a popular benchmark testcase for viscoelasic fluids. The sharp contraction leads to a geometrical singularity at the re-entrant corner, where stresses tend to infinity. This offers a challenge for the numerical simulation and the testcase is used in order to prove the stability of the numerical approach. It has been extensively studied in literature for isothermal flow conditions.[9,11,13,16]

The first attempt to model the temperature dependence of viscoelastic flow variables was the time-temperature superposition principle. In this theory, one empirical equation is used to describe the temperature-dependent behavior of all mechanical relaxation processes.[1] With this principle it is possible to predict the characteristics of the flow at a specific temperature using the values at another temperature. However, with this approach it is not possible to describe the spatial and temporal temperature dependence of the flow field.[6] To overcome this limitation the method was extended to the so-called "pseudo time approach". By introducing a virtual time that depends both upon the real time and the spatial variable, it becomes possible to solve the system for the virtual time. Temporal and spatial inhomogenities in temperature are included implicitly.[2] Yet the approach draws strong limitions regarding the fluid type and requires very small temperature variations, so that it is only applicable to a limited amount of practical cases.[12]

In the 1990s, much more general theories were found. Starting from traditional thermodynamics, Braun[7] developed a set of equations to model the non-isothermal behavior of a special group of viscoelastic fluids. Peters and Baaijens[8] derived non-isothermal formulations for the PTT-model equations. They numerically simulated the benchmark case of a flow past a confined cylinder. Wachs and Clermont[14] extended the framework to the UCM fluid model and used it to simulate an axisymmetric 4:1 contraction flow with cooled walls. Habla et al.[20] used the same framework for an Oldroyd-B fluid to solve the 4:1 axisymmetric flow with heated and cooled walls.

This paper is organised as follows: in the next section the governing balance equations and the thermorheological modelling are outlined.

The consecutive section gives an overview of the numerical setup and the boundary conditions. Section RESULTS AND DISCUSSION presents some key results for the planar 4:1 contraction flow with heated/cooled walls. The last section concludes with a discussion of the results and a short outlook to future work.

GOVERNING EQUATIONS

The balance equations for a non-isothermal viscoelastic fluid are presented.

Mass and Momentum balance

Assuming incompressiblity, the mass balance simplifies to

$$\nabla \cdot \mathbf{V} = 0.$$

The momentum balance reads

$$\frac{\partial \rho \mathbf{V}}{\partial t} + (\nabla \cdot \rho \mathbf{V}\mathbf{V}) + \nabla p - (\nabla \cdot \tau) = 0$$

with density ρ, velocity vector $\mathbf{V}$, time t, pressure p and stress tensor τ. The stress tensor is modelled using the Oldroyd-B model in solvent-polymer stress splitting formulation (SPSS) introduced by Bird.[5]

$$\tau = \tau_{\mathbf{s}} + \tau_{\mathbf{p}}$$

The idea is to split the stress tensor into a newtonian "solvent" part $\tau_{\mathbf{s}} = 2\eta_s \mathbf{D}$ with the solvent viscosity η_s and a polymeric part $\tau_{\mathbf{p}}$. For the polymeric part, a constitutive equation is introduced to model the temporal dependence on stress history

$$\tau_{\mathbf{p}} + \lambda \overset{\triangledown}{\tau}_{\mathbf{p}} = 2\eta_p \mathbf{D}.$$

Here λ is the relaxation time, η_p the polymeric viscosity and $\mathbf{D}$ is the deformation rate tensor defined as

$$\mathbf{D} = \frac{1}{2}\left[\nabla \mathbf{V} + (\nabla \mathbf{V})^T\right].$$

$\overset{\triangledown}{\tau}_{\mathbf{p}}$ is the upper-convected time derivative of the polymeric stress tensor.

Thermorheological Modelling

The thermorheological modelling of the Oldroyd-B fluid is following the work of Peters and Baaijens.[8] The balance equation for internal energy is

$$\frac{\partial \rho e}{\partial t} + (\nabla \cdot \rho \mathbf{V} e) + \nabla \cdot \mathbf{q} + Q = 0$$

with internal energy e, heat flux $\mathbf{q}$ and energy source term Q. The heat flux is modelled using Fourier's law

$$\mathbf{q} = -k \nabla T.$$

The internal energy of a viscoelastic fluid is in general dependent upon temperature and a strain tensor, which changes the internal source term. Introducing this dependence into the second law of thermodynamics, two extreme cases for the source term can be derived: If the internal energy depends upon temperature only ($u = u(T)$) all internally produced energy is viscously dissipated. This case is generally referred to as pure entropy elasticity. The transformation is irreversible and producing entropy only. The other extreme is that entropy is a function of temperature only ($s = s(T)$). In this case all mechanical energy is elastically stored and no entropy is produced at all. It is commonly referred to as pure energy elasticity. The ratio of entropy to energy elasticity is dependent upon the local flow situation.[18] A simplifying approach is the definition of an a priori splitting factor α, which was proposed by Peters and Baaijens,[8] with $0 < \alpha < 1$. $\alpha = 0$ means pure energy elasticity, while $\alpha = 1$ is pure entropy elasticity. With this approach, the energy source term can be modelled as

$$Q = \tau_{\mathbf{s}} : \mathbf{D} + \alpha \tau_{\mathbf{p}} : \mathbf{D} + (1-\alpha)\frac{tr(\tau_{\mathbf{p}})}{2\lambda(T)}.$$

Experiments show that viscosity and relaxation time exhibit a significant dependence upon temperature. For polymer melts, this dependence is commonly modelled by the empirical William-Landel-Ferry (WLF) formulation.[1] The shift factor a_T is introduced to relate values

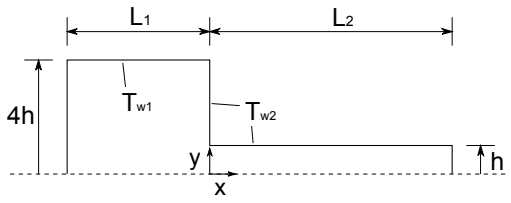

Figure 1. Geometry of the planar contraction

at the current temperature to those at a reference temperature T_0.

$$\eta_{s/p}(T) = a_T \eta_{s/p}(T_0)$$

$$\lambda(T) = a_T \lambda(T_0)$$

$$log(a_T) = \frac{c_1(T-T_0)}{c_2+T-T_0}$$

c_1 and c_2 are material-dependent constants.

NUMERICAL SETUP

For this numerical study, an in-house block-structured parallelized Finite-Volume solver is used. The coupled set of constitutive equations is solved by a decoupled iterative approach, based on the SIMPLE algorithm.[4]

Stabilization for the constitutive equation of the extra stress tensor is achieved by using the square root conformation representation proposed by Balci et al.[19] In order to cope with the high viscosities, the momentum balance equation is stabilized by the both sides diffusion approach (see for example[10]).

Geometry

A planar contraction flow of ratio 4:1 is investigated. Figure 1 presents a sketch of the considered geometry. The length of the inflow duct is $L_1 = 20h$, while the length of the outflow duct $L_2 = 50h$ is chosen much longer, so that velocity and temperature profiles can fully develop. For the non-isothermal testcases, the wall of the contraction corner and the outflow duct can be heated or cooled in comparison to the wall of the inflow duct.

Boundary conditions

At the inlet Dirichlet boundary conditions are prescribed for temperature and velocity. The temperature is constant and equal to the wall temperature of the inflow duct. A parabolic velocity profile is prescribed with a mean velocity of $\overline{V_1} = 0.00129\frac{m}{s}$. Zero gradient boundary conditions are used for the extra stress tensor and pressure. At the outlet, zero gradient boundary conditions are prescribed for velocity, extra stress tensor and temperature. A Dirichlet boundary condition is used for pressure. No-slip conditions are assumed at the walls for velocity, the wall temperature is constant. The wall temperature of the contraction corner and outlet duct can be varied compared to the inlet duct wall temperature. The amounts of heating or cooling are denoted by ΔT. For the extra stress tensor no boundary conditions are necessary as the constitutive equation is of hyperbolic type. For the discretization of the fluxes however, the values at the wall are needed. They are calcutated by extrapolation using the stress values in the two control volumes nearest to the wall.

fluid	properties	temperature	
ρ	$921\frac{kg}{m^3}$		
η_0	$10^4\frac{kg}{ms}$	T_i	$462K$
λ	$0.1s$	$T_{w,1}$	T_i
c_p	$1500\frac{J}{kgK}$	$T_{w,2}$	$T_{w,1}+\Delta T$
k	$0.17\frac{W}{mK}$		

Table 1. Fluid properties and temperature boundary conditions

Fluid property values are chosen in the style of Wachs Clermont,[14] they are summarized in table 1. The ratio of solvent to polymeric viscosity is set to $1/19$.

In order to investigate grid sensitivity, three different meshes are considered that are successively refined towards the singularity. Table 2 provides an overview of the mesh parameters.

grid	control volumes	$\Delta x_{min}/h = \Delta y_{min}/h$
mesh 01	10314	0.02
mesh 02	27830	0.01
mesh 03	65926	0.005

Table 2. Mesh parameters

RESULTS AND DISCUSSION

Calculations were performed under isothermal and non-isothermal flow conditions. Some results are presented in the following section.

Dimensionless numbers and field variables

Dimensionless numbers are used to characterize and compare the flow behavior. The Reynolds-Number describes the ratio of inertial to viscous forces. For the presented flow it is defined as

$$Re = \frac{\overline{\mathbf{V}_{x,2}} h \rho}{\eta_0},$$

where $\overline{\mathbf{V}_{x,2}}$ is the integrated mean velocity in the outflow duct. In the investigated testcases the Reynolds-Number has a value of $Re = 4.74e^{-04}$, which corresponds to creeping flow conditions.

The Weissenberg-Number characterizes the ratio of elastic to viscous forces

$$Wi = \frac{\lambda \overline{\mathbf{V}_{x,2}}}{h}.$$

All the presented calculations were performed with a relaxation time $\lambda = 0.1s$, which corresponds to a Wi-Number of $Wi = 5.16e^{-04}$. At this small value elastic effects are not very pronounced, so that the dependence of the flow field on time is still almost negligible. In order to test the algorithm, steady-state calculations were performed which were observed to be in good agreement with the unsteady solution for this Wi-Number. In literatue the Deborah-Number is sometimes used instead of the Wi-Number. The Deborah-Number De is defined as the ratio of the "time of relaxation" to "time of observation".[3] Small values thus characterize a more "fluid-like" behavior, large values a more pronounced "solid-like" or elastic behavior of the viscoelastic material.

For better comparison velocities and stresses are plotted in dimensionless form in the style of Habla et al.[20] The velocity is normalized with the mean velocity in the outlet duct

$$\widetilde{\mathbf{V}}_i = \frac{\mathbf{V}_i}{\overline{\mathbf{V}_{x,2}}}.$$

The polymeric stress tensor in its dimensionless form is

$$\widetilde{\tau_{p,ij}} = \frac{\tau_{p,ij} h}{\overline{\mathbf{V}_{x,2}} \eta_0}$$

with the corresponding axis directions i and j.

Isothermal testcase

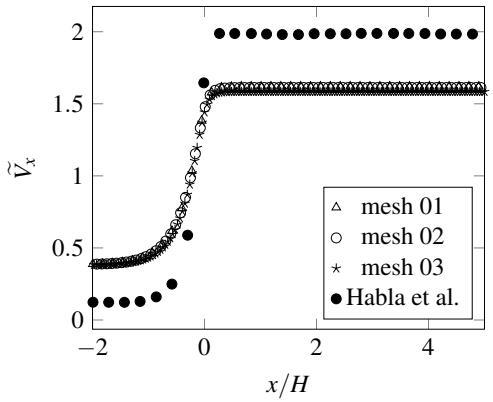

Figure 2. Dimensionless velocity at the centerline for three different meshes at $\lambda = 0.1$; data from Habla et al. at $De = 0$

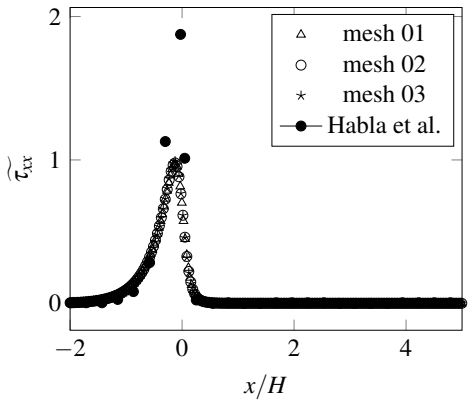

Figure 3. Dimensionless stress profile for three different meshes for $\lambda = 0.1$; data from Habla et al. at $De = 0$

Figure 2 shows the normalized velocity in axial direction at the centerline $y = 0$. Results from Habla et al.[20] at a De-Number of $De = 0$ are plotted for comparison. The curves are in good qualitative agreement, however they show differences in the level values and the slope of the velocity rise. This can be explained when considering the geometry of the testcase. The

literature data was obtained in an axisymmetric testcase, while the case investigated in the present paper is planar. When considering the mass flux balance $\dot{m} = \rho \overline{\mathbf{V}} A$ and taking into account incompressibility, the ratio of velocities in inflow to outflow duct is a function of the geometry only: $\overline{\mathbf{V}_2}/\overline{\mathbf{V}_1} = A_1/A_2$. In the axisymmetric case this leads to a velocity ratio of $1/16$, while only to a ratio of $1/4$ in the planar case. Starting from the same mean velocity at the inlet, the inlet velocity in the planar testcase is normalized by a smaller value, so that its dimensionless value is larger than in the axisymmetric case (about 0.4 compared to 0.15 for the axisymmetric testcase). Again starting from the same mean inflow velocity, the rise in velocity at the contraction is higher in the axisymmetric case, where a value of 2 is reached while only 1.6 in the present planar testcase. Nigen and Walters[15] experimentally investigated an axisymmetric and a planar contraction flow of the same contraction ratio. They observed, when comparing the velocity magnitude at the centerline for the planar and the axisymmetric contraction flow, that the velocity rise in the planar testcase was clearly smaller than in the axisymmetric one, which underlines the results found in the present study.

Figure 3 shows the normalized stress profile at the center line for three different meshes. Literature data from Habla et al.[20] are plotted for comparison. The curves are in good qualitative aggreement, though it is clearly visible that the peak values differ significantly. The explanation is similar as for the velocity. Since the mean outlet velocity is used for normalization of the stress profile, this is expected to be smaller than in the axisymmetric case, which is in accordance with the presented results.

In figure 4 the mean outflow velocity is plotted against the number of control volumes for all three meshes. The results differ only in the fifth decimal digit and follow a trend towards one value, so the conclusion is drawn that all meshes lay within the asymptotic regime. All consecutive calculations are performed with mesh 03.

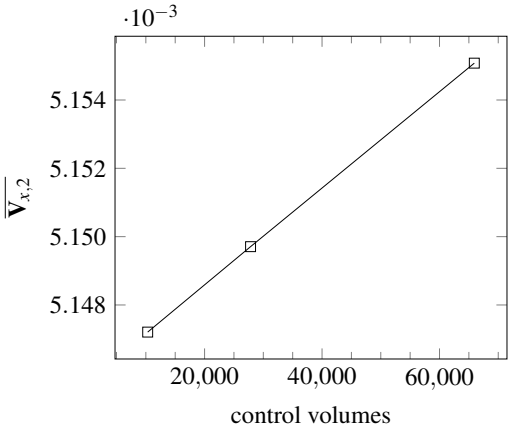

Figure 4. Mean velocity in the outlet duct in dependence of the number of control volumes

Non-isothermal testcase

In the upper corner of the contraction a recirculation zone develops. Its size is dependent upon the Wi-Number and in the non-isothermal case also upon the amount of heating or cooling of the wall.[14]

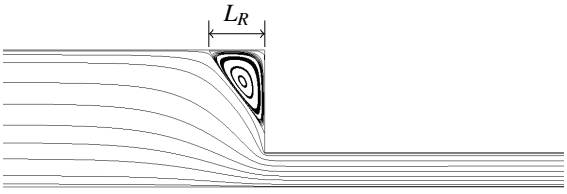

Figure 5. Recirculation zone for $\Delta T = 10K$

In Figure 5 the flow field with the recirculation zone is visualized through streamtraces at a $\Delta T = 10K$. L_R denotes the size of the recirculation zone. For better comparison, it is dimensionalized by the size of the inflow duct $\chi = \frac{L_R}{2 \cdot 4h}$, χ being the dimensionless vortex size. Figure 6 shows the dimensionless vortex size depending on the amount of heating or cooling of the wall. The results are plotted for an energy partitioning factor $\alpha = 1$ and $\alpha = 0$. Habla et al.[20] found a value of $\chi = 0.22$ at a Deborah-Number of $De = 1$ for the smallest dimensionless vortex at $\Delta T = 30K$. Since the vortex size grows with increasing De-Number, the results shown here were expected to be smaller. The increase in vortex size with higher wall temperatures is clearly visible and following the same trend as in the literature data.

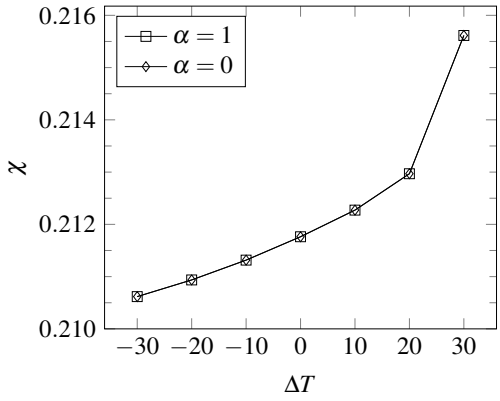

Figure 6. Dimensionless vortex length in dependence of ΔT for energy partitioning factor $\alpha = 0$ and $\alpha = 1$

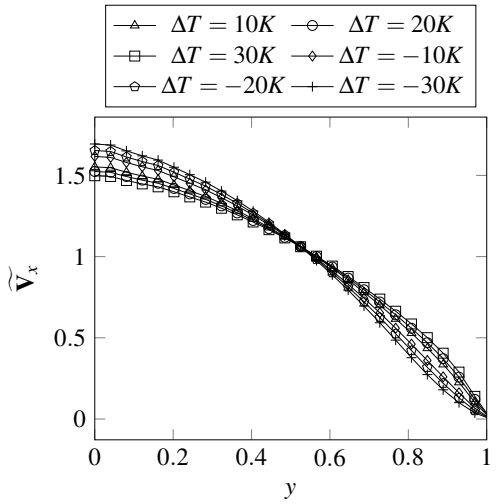

Figure 7. Dimensionless velocity profile at the outlet dependent on ΔT

Figure 7 shows the dimensionless outlet velocity profile for different amounts of heating or cooling of the walls.

SUMMARY AND CONCLUSIONS

A planar 4:1 contraction flow of an Oldroyd-B fluid was investigated numerically with an in-house Finite-Volume solver. The thermorheological behavior of the viscoelastic fluid was modeled following an approach from Peters and Baaijens.[8] The calculations were performed at a very small Wi-Number where elastic effects of the fluid are comparably small and steady-state solutions can give a reasonable insight into the flow characteristica.
For isothermal flow conditions the dimensionless stress and velocity profile at the centerline were investigated and found to be in reasonable agreement with literature data. The differences to literature data were expected and can be adressed to the different choice in geometry. In the non-isothermal testcases, the walls of the contraction corner and the outlet duct can be heated or cooled compared to the fluid temperature. The size of the recirculation zone is dependent upon Wi-Number (which was kept constant) and temperature. The recirculation zone was investigated for different amounts of heating or cooling at either pure energy elasticity or pure entropy elasticity.
When increasing the Wi-Number, the time-dependence of the problem becomes clearly more pronounced, so that a steady-state solution can no longer provide insight into the flow behavior. The presented calculations should serve to test the implementation of the thermorheological modelling. The next step will be to investigate the flow behavior at increasing Weissenberg Numbers.

ACKNOWLEDGEMENTS

The work of Stefanie Meburger is supported by the 'Excellence Initiative' of the German Federal and State Governments and the Graduate School of Computational Engineering at Technische Universität Darmstadt.

REFERENCES

1. Williams, M. L., Landel, R. F. and Ferry, J. D. (1955), "The temperature dependence of relaxation mechanisms in amorphous polymers and other glass-forming liquids", *Journal of the American Chemical Society*, **77**, 3701–3707.

2. Morland, L. W. and Lee, E. (1960), "Stress analysis for linear viscoelastic materials with temperature variation", *Transactions of the Society of Rheology*, **4**, 233–263.

3. Reiner, M. (1964), "The deborah number", *Physics today*, **17**, 62.

4. Patankar, S. V. and Spalding, D. B. (1972), "Numerical prediction of three-dimensional flows", Imperial College of Science and Technology, Mechanical Engineering Department.

5. Bird, R. B., Armstrong, R. C. and Hassager, O.

(1987), "Dynamics of polymeric liquids. Vol. 1: Fluid mechanics", John Wiley and Sons Inc., New York, NY.

6. Wiest, J. M. (1988), "Time-temperature superposition in nonisothermal flow", *Journal of Non-Newtonian Fluid Mechanics*, **27**, 127–131.

7. Braun, H. (1991), "A model for the thermorheological behavior of viscoelastic fluids", *Rheologica Acta*, **30**, 523–529.

8. Peters, G. W. and Baaijens, F. P. (1997), "Modelling of non-isothermal viscoelastic flows", *Journal of Non-Newtonian Fluid Mechanics*, **68**, 205–224.

9. Mompean, G. and Deville, M. (1997), "Unsteady finite volume simulation of Oldroyd-B fluid through a three-dimensional planar contraction", *Journal of Non-Newtonian Fluid Mechanics*, **72**, 253–279.

10. Oliveira, P., Pinho, F. T. d. and Pinto, G. (1998), "Numerical simulation of non-linear elastic flows with a general collocated finite-volume method", *Journal of Non-Newtonian Fluid Mechanics*, **79**, 1–43.

11. Matallah, H., Townsend, P. and Webster, M. (1998), "Recovery and stress-splitting schemes for viscoelastic flows", *Journal of Non-Newtonian Fluid Mechanics*, **75**, 139–166.

12. Dressler, M., Edwards, B. J. and Öttinger, H. C. (1999), "Macroscopic thermodynamics of flowing polymeric liquids", *Rheologica Acta*, **38**, 117–136.

13. Alves, M., Pinho, F. and Oliveira, P. (2000), "Effect of a high-resolution differencing scheme on finite-volume predictions of viscoelastic flows", *Journal of Non-Newtonian Fluid Mechanics*, **93**, 287–314.

14. Wachs, A. and Clermont, J.-R. (2000), "Non-isothermal viscoelastic flow computations in an axisymmetric contraction at high Weissenberg numbers by a finite volume method", *Journal of Non-Newtonian Fluid Mechanics*, **95**, 147–184.

15. Nigen, S. and Walters, K. (2002), "Viscoelastic contraction flows: comparison of axisymmetric and planar configurations", *Journal of Non-Newtonian Fluid Mechanics*, **102**, 343–359.

16. Kim, J. M., Kim, C., Kim, J. H., Chung, C., Ahn, K. H. and Lee, S. J. (2005), "High-resolution finite element simulation of 4: 1 planar contraction flow of viscoelastic fluid", *Journal of Non-Newtonian Fluid Mechanics*, **129**, 23–37.

17. Wilson, H. J. (2006), "Instabilities and constitutive modelling", *Philosophical Transactions of the Royal Society of London A: Mathematical, Physical and Engineering Sciences*, **364**, 3267–3283.

18. Hütter, M., Luap, C. and Öttinger, H. C. (2009), "Energy elastic effects and the concept of temperature in flowing polymeric liquids", *Rheologica Acta*, **48**, 301–316.

19. Balci, N., Thomases, B., Renardy, M. and Doering, C. R. (2011), "Symmetric factorization of the conformation tensor in viscoelastic fluid models", *Journal of Non-Newtonian Fluid Mechanics*, **166**, 546–553.

20. Habla, F., Woitalka, A., Neuner, S. and Hinrichsen, O. (2012), "Development of a methodology for numerical simulation of non-isothermal viscoelastic fluid flows with application to axisymmetric 4: 1 contraction flows", *Chemical Engineering Journal*, **207**, 772–784.